Simulation Models With Correct Statistical Properties for Rayleigh Fading Channels

Yahong Rosa Zheng and Chengshan Xiao, *Senior Member, IEEE*

***Abstract*—In this paper, new sum-of-sinusoids statistical simulation models are proposed for Rayleigh fading channels. These new models employ random path gain, random initial phase, and conditional random Doppler frequency for all individual sinusoids. It is shown that the autocorrelations and cross correlations of the quadrature components, and the autocorrelation of the complex envelope of the new simulators match the desired ones exactly, even if the number of sinusoids is as small as a single-digit integer. Moreover, the probability density functions of the envelope and phase, the level crossing rate, the average fade duration, and the autocorrelation of the squared fading envelope which contains fourth-order statistics of the new simulators, asymptotically approach the correct ones as the number of sinusoids approaches infinity, while good convergence is achieved even when the number of sinusoids is as small as eight. The new simulators can be directly used to generate multiple uncorrelated fading waveforms for frequency selective fading channels, multiple-input multiple-output channels, and diversity combining scenarios. Statistical properties of one of the new simulators are evaluated by numerical results, finding good agreements.**

***Index Terms*—Channel models, fading channel simulator, fading channels, high-order statistics, Rayleigh fading, second-order statistics.**

I. Introduction

MOBILE radio channel simulators are commonly used in the laboratory because they allow system tests and evaluations which are less expensive and more reproducible than field trials. Many different approaches have been used for the modeling and simulation of mobile radio channels [1]–[23], [31], [32]. Among them, the well-known mathematical reference model due to Clarke [1] and its simplified simulation model due to Jakes [6] have been widely used for Rayleigh fading channels for about three decades. However, Jakes' simulator is a deterministic model, and it has difficulty in creating multiple uncorrelated fading waveforms for frequency-selective fading channels and multiple-input multiple-output (MIMO) channels, therefore, different modifications of Jakes' simulator have been reported in the literature [10], [16]–[19], [31]. Despite the extensive acceptance and application of Jakes' simulator, some important limitations of the simulator were determined and discussed in detail recently [22]. It was shown in [22] that Jakes' simulator is wide-sense nonstationary when averaged across the physical ensemble of fading channels. Pop and Beaulieu [22] proposed an improved simulator by introducing random phase shifts in the low-frequency oscillators to remove the stationary problem. However, it was pointed out in [22] that higher-order statistics of this improved simulator may not match the desired ones. Consistent with Pop and Beaulieu's caution about higher-order statistics of the improved simulator, it was further proved in [24] that second-order statistics of the quadrature components and the envelope do not match the desired ones. Moreover, even in the limit as the number of sinusoids approaches infinity, the autocorrelations and cross correlations of the quadrature components, and the autocorrelation of the squared envelope of the improved simulator, fail to match the desired correlations. Jakes' original simulator and published modified versions of it, have similar problems with these second-order statistics.

In this paper, new sum-of-sinusoids statistical simulation models are proposed for Rayleigh fading channels. It is shown that the autocorrelations and cross correlations of the quadrature components, and the autocorrelation of the complex envelope of the new simulators, match the desired ones exactly even if the number of sinusoids is so small as a single-digit integer. Furthermore, the autocorrelation of the squared envelope which contains fourth-order statistics, the probability density functions (PDFs) of the fading envelope and the phase, the level-crossing rate, and the average fade duration of our new simulators asymptotically approach the desired ones as the number of sinusoids approaches infinity. Moreover, convergence to the limiting (exact) values of these properties, except for the fading phase's PDF, is rapid and close approximation is achieved even when the number of sinusoids is as small an integer as eight, and the number of random trials is only 50. Additionally, and importantly, the new simulator can be directly used to generate multiple uncorrelated fading waveforms, which are needed to simulate some realistic frequency-selective fading channels, MIMO channels, and diversity-combining scenarios.

The remainder of this paper is organized as follows. Section II briefly reviews the mathematical reference model and the family of Jakes' simulators. Attention is given to the statistical properties of the reference model and an improved Jakes simulator. Section III proposes a new sum-of-sinusoids simulation model for Rayleigh fading channels, and the statistical properties of

Paper approved by R. A. Valenzuela, the Editor for Transmission Systems of the IEEE Communications Society. Manuscript received April 1, 2002; revised November 7, 2002. This work was supported in part by the University of Missouri (UM)-Columbia Research Council under Grant URC-02-050 and in part by the UM System Research Board under Grant URB-02-124. This paper was presented in part at the IEEE Vehicular Technology Conference, Birmingham, AL, May 6–9, 2002.

The authors are with the Department of Electrical and Computer Engineering, University of Missouri, Columbia, MO 65211 USA (e-mail: yzheng@ee.missouri.edu; xiaoc@missouri.edu).

Digital Object Identifier 10.1109/TCOMM.2003.813259

this new model are analyzed in detail. Other models with identical or similar statistical properties are also briefly discussed in this section. Section IV presents the performance evaluation of one of the new simulators by extensive numerical results. Section V draws some conclusions.

II. Reference Model and Jakes' Simulator Family

A. Mathematical Reference Model

Consider a frequency-nonselective fading channel comprised of N propagation paths; the low-pass fading process is given by [1] and [6]

$$g(t) = E_0 \sum_{n=1}^{N} C_n \exp\left[j(w_d t \cos\alpha_n + \phi_n)\right] \tag{1}$$

where E_0 is a scaling constant, C_n, α_n, and ϕ_n are, respectively, the random path gain, angle of incoming wave, and initial phase associated with the nth propagation path, and w_d is the maximum radian Doppler frequency occurring when $\alpha_n = 0$.

Assuming that C_n is real valued, (1) can be written as

$$g(t) = g_c(t) + jg_s(t) \tag{2a}$$

$$g_c(t) = E_0 \sum_{n=1}^{N} C_n \cos(w_d t \cos\alpha_n + \phi_n) \tag{2b}$$

$$g_s(t) = E_0 \sum_{n=1}^{N} C_n \sin(w_d t \cos\alpha_n + \phi_n). \tag{2c}$$

The central limit theorem justifies that $g_c(t)$ and $g_s(t)$ can be approximated as Gaussian random processes for large N. Assuming that α_n and ϕ_n are mutually independent and uniformly distributed over $[-\pi, \pi)$ for all n, and adopting Clarke's two-dimensional (2-D) isotropic scattering model, some desired second-order statistics for fading simulators are manifested in the autocorrelation and cross-correlation functions [1], [25]

$$R_{g_c g_c}(\tau) = E\left[g_c(t) g_c(t+\tau)\right] = J_0(w_d\tau) \tag{3a}$$

$$R_{g_s g_s}(\tau) = J_0(w_d\tau) \tag{3b}$$

$$R_{g_c g_s}(\tau) = 0 \tag{3c}$$

$$R_{g_s g_c}(\tau) = 0 \tag{3d}$$

$$R_{gg}(\tau) = E\left[g(t) g^*(t+\tau)\right] = 2J_0(w_d\tau) \tag{3e}$$

$$R_{|g|^2|g|^2}(\tau) = 4 + 4J_0^2(w_d\tau) \tag{3f}$$

where $E[\cdot]$ denotes expectation, $J_0(\cdot)$ is the zero-order Bessel function of the first kind [26], and without loss of generality, we have set $\sum_{n=0}^{N} E[C_n^2] = 1$ and $E_0 = \sqrt{2}$. The first-order PDFs of the fading envelope, $|g(t)|$, and the phase, $\Theta_g(t) = \arctan\left[g_c(t), g_s(t)\right]$[1],[1] are given by

$$f_{|g|}(x) = x \cdot \exp\left(-\frac{x^2}{2}\right), \qquad x \geq 0 \tag{4a}$$

$$f_{\Theta_g}(\theta_g) = \frac{1}{2\pi}, \qquad \theta_g \in [-\pi, \pi). \tag{4b}$$

[1]The function arctan(x, y) maps the arguments (x, y) into a phase in the correct quadrant in $[-\pi, \pi)$.

Clearly, the fading envelope $|g|$ is Rayleigh distributed according to (4a), and the phase $\Theta_g(t)$ is uniformly distributed.

B. Jakes' Simulator Family

Based on Clarke's reference model (1), and by selecting

$$C_n = \frac{1}{\sqrt{N}} \tag{5a}$$

$$\alpha_n = \frac{2\pi n}{N}, \qquad n = 1, 2, \ldots, N \tag{5b}$$

$$\phi_n = 0, \qquad n = 1, 2, \ldots, N. \tag{5c}$$

Jakes derived his well-known simulation model for Rayleigh fading channels. The normalized low-pass fading process of this model is given by

$$\bar{u}(t) = \bar{u}_c(t) + j\bar{u}_s(t) \tag{6a}$$

$$\bar{u}_c(t) = \frac{2}{\sqrt{N}} \sum_{n=0}^{M} a_n \cos(w_n t) \tag{6b}$$

$$\bar{u}_s(t) = \frac{2}{\sqrt{N}} \sum_{n=0}^{M} b_n \cos(w_n t) \tag{6c}$$

where $N = 4M + 2$, and

$$a_n = \begin{cases} \sqrt{2}\cos\beta_0, & n = 0 \\ 2\cos\beta_n, & n = 1, 2, \ldots, M \end{cases} \tag{7a}$$

$$b_n = \begin{cases} \sqrt{2}\sin\beta_0, & n = 0 \\ 2\sin\beta_n, & n = 1, 2, \ldots, M \end{cases} \tag{7b}$$

$$\beta_n = \begin{cases} \frac{\pi}{4}, & n = 0 \\ \frac{\pi n}{M}, & n = 1, 2, \ldots, M \end{cases} \tag{7c}$$

$$w_n = \begin{cases} w_d, & n = 0 \\ w_d \cos\frac{2\pi n}{N}, & n = 1, 2, \ldots, M. \end{cases} \tag{7d}$$

The simplifying relationships forced in (5) make this simulation model deterministic [10], [16] and wide-sense nonstationary [22]. Therefore, various modifications of Jakes' simulator have been proposed in [10], [16]–[19], [21], [22], [31] and the references therein, which we call the family of Jakes' simulators. Among the Jakes simulator family, the recently improved model proposed by Pop and Beaulieu in [22] is worthy of mention due to its wide-sense stationarity.

The normalized low-pass fading process of the improved Jakes'simulator proposed in [22] is given by

$$u(t) = u_c(t) + ju_s(t) \tag{8a}$$

$$u_c(t) = \frac{2}{\sqrt{N}} \sum_{n=0}^{M} a_n \cos(w_n t + \phi_n) \tag{8b}$$

$$u_s(t) = \frac{2}{\sqrt{N}} \sum_{n=0}^{M} b_n \cos(w_n t + \phi_n) \tag{8c}$$

where a_n, b_n, β_n, and w_n are the same as those of Jakes' original model given by (7), and ϕ_n are independent random variables uniformly distributed on $[-\pi, \pi)$ for all n.

Clearly, the difference between this improved simulator and Jakes' original simulator lies in the random phases ϕ_n, $n = 0, 1, \ldots, M$, as the original Jakes simulator assumes that $\phi_n = 0$ for all n. The introduction of these random phases ϕ_n

eliminates the stationarity problem occurring in Jakes' original design. However, some problems with higher-order statistics remain.

Some second-order statistics of the improved Jakes model are given by [24]

$$R_{u_cu_c}(\tau)=\frac{4}{N}\left[\sum_{n=0}^{M}\frac{a_n^2}{2}\cdot\cos(w_n\tau)\right] \tag{9a}$$

$$R_{u_su_s}(\tau)=\frac{4}{N}\left[\sum_{n=0}^{M}\frac{b_n^2}{2}\cdot\cos(w_n\tau)\right] \tag{9b}$$

$$R_{u_cu_s}(\tau)=\frac{4}{N}\left[\sum_{n=0}^{M}\frac{a_nb_n}{2}\cdot\cos(w_n\tau)\right] \tag{9c}$$

$$R_{u_su_c}(\tau)=R_{u_cu_s}(\tau) \tag{9d}$$

$$R_{uu}(\tau)=\frac{4}{N}\left[\sum_{n=1}^{M}2\cos(w_n\tau)+\cos(w_d\tau)\right] \tag{9e}$$

$$R_{|u|^2|u|^2}(\tau)=4+2R_{u_cu_c}^2(\tau)+2R_{u_su_s}^2(\tau)+4R_{u_cu_s}^2(\tau)+\frac{8}{N}J_0(2w_d\tau)+\frac{16(N-1)}{N^2} \tag{9f}$$

where $R_{u_cu_c}(\tau)$ and $R_{u_su_s}(\tau)$ are the autocorrelations of the quadrature components, $R_{u_cu_s}(\tau)$ and $R_{u_su_c}(\tau)$ are the cross correlations of the quadrature components, and $R_{uu}(\tau)$ and $R_{|u|^2|u|^2}(\tau)$ are the autocorrelations of the complex envelope and the squared envelope, respectively. Although the autocorrelation of the complex envelope $R_{uu}(\tau)$ approaches the desired autocorrelation $R_{gg}(\tau)$ when M approaches infinity, it is clear by comparing (9) with (3) that all the second-order statistics shown in (9) do not match the desired ones. Moreover, even in the limit as the number of sinusoids approaches infinity, the autocorrelations and cross correlations of the quadrature components and the autocorrelation of the squared envelope of the improved simulator fail to match the desired statistics [24]. Jakes' original model and its existing modifications [10], [16]–[19], [21], [31] have similar shortcomings with respect to these aforementioned statistics.

III. New Simulation Models

In this section, an improved simulation model is proposed by reintroducing the randomness for all three random variables C_n, α_n, and ϕ_n. Statistical properties of the proposed model are analyzed. It is shown that second-order correlation statistics of the proposed model match the desired ones exactly even if the number of sinusoids is small; fourth-order statistics of the new model asymptotically match the correct ones as the number of sinusoids approaches infinity. Moreover, other models which have identical or similar statistical properties to that of the proposed model are presented. The application of the proposed model to generating multiple uncorrelated fading waveforms is discussed as well.

To properly introduce randomness to C_n, α_n, and ϕ_n, we consider the following simulation prototype function:

$$\tilde{g}(t)=E_0\sum_{n=1}^{N}\tilde{C}_n\exp\left\{j(w_dt\cos\tilde{\alpha}_n+\tilde{\phi}_n)\right\} \tag{10}$$

where

$$\tilde{C}_n=\frac{\exp(j\psi_n)}{\sqrt{N}},\qquad n=1,2,\ldots,N \tag{11a}$$

$$\tilde{\alpha}_n=\frac{2\pi n-\pi+\theta}{N},\qquad n=1,2,\ldots,N \tag{11b}$$

$$\tilde{\phi}_n=-\tilde{\phi}_{\frac{N}{2}+n}=\phi,\qquad n=1,2,\ldots,\frac{N}{2} \tag{11c}$$

with $N/2$ being an integer, and ψ_n, θ, and ϕ being mutually independent random variables uniformly distributed on $[-\pi,\pi)$.

For this prototype function, it is easy to verify that $|\tilde{C}_n|=C_n$, i.e., the amplitude of the complex-valued path gain is equal to the real-valued path gain given by (5a). It is pointed out that $\tilde{C}_n$ and $\tilde{\phi}_n$ have one redundant random phase which is needed for our new model. It will be explained later in this section. The reintroduced randomness for $\tilde{C}_n$, $\tilde{\alpha}_n$, and ϕ_n, rather than those given in (5a), enables us to establish a new statistical and wide-sense stationary (WSS) simulation model for Rayleigh fading channels.

Slightly different from Jakes' simplification procedure described in [6, p. 68] and [25, p. 82], we choose $\psi_{N/2+n}=\psi_n$, then (10) can be rearranged to give

$$\tilde{g}(t)=\frac{E_0}{\sqrt{N}}\left\{\sum_{n=1}^{\frac{N}{2}}e^{j\psi_n}\left[e^{j(w_dt\cos\tilde{\alpha}_n+\phi)}+e^{-j(w_dt\cos\tilde{\alpha}_n+\phi)}\right]\right\}. \tag{12}$$

The first term in the sums represents waves with radian Doppler frequencies that progress from the range of $[w_d\cos(2\pi/N),w_d]$ to the range of $[-w_d\cos(2\pi/N),-w_d]$, while the radian Doppler frequencies in the second term of the sums shift from the range of $[-w_d\cos(2\pi/N),-w_d]$ to the range of $[w_d\cos(2\pi/N),w_d]$. Therefore, the Doppler frequencies in these terms are overlapped. To represent the fading signals whose Doppler frequencies do not overlap, $\tilde{g}(t)$ can be further simplified to be

$$\hat{g}(t)=\frac{E_0}{\sqrt{N}}\left\{\sum_{n=1}^{M}\sqrt{2}e^{j\psi_n}\left[e^{j(w_nt+\phi)}+e^{-j(w_nt+\phi)}\right]\right\} \tag{13}$$

where $M=N/4$, and $w_n=w_d\cos\tilde{\alpha}_n$. The factor $\sqrt{2}$ is included to make the total power remain unchanged. Based on $\hat{g}(t)$, we can define a new simulation model as follows.

Definition: The normalized low-pass fading process of a new statistical sum-of-sinusoids simulation model is defined by

$$X(t)=X_c(t)+jX_s(t) \tag{14a}$$

$$X_c(t)=\frac{2}{\sqrt{M}}\sum_{n=1}^{M}\cos(\psi_n)\cdot\cos(w_dt\cos\alpha_n+\phi) \tag{14b}$$

$$X_s(t)=\frac{2}{\sqrt{M}}\sum_{n=1}^{M}\sin(\psi_n)\cdot\cos(w_dt\cos\alpha_n+\phi) \tag{14c}$$

with

$$\alpha_n=\frac{2\pi n-\pi+\theta}{4M},\qquad n=1,2,\ldots,M \tag{15}$$

where θ, ϕ, and ψ_n are statistically independent and uniformly distributed over $[-\pi,\pi)$ for all n.

We now present the correlation statistics of the fading signal $X(t)$ in the following theorem.

Theorem 1: The autocorrelation and cross-correlation functions of the quadrature components, and the autocorrelation functions of the complex envelope and the squared envelope of the fading signal $X(t)$ are given by

$$R_{X_cX_c}(\tau) = J_0(w_d\tau) \tag{16a}$$
$$R_{X_sX_s}(\tau) = J_0(w_d\tau) \tag{16b}$$
$$R_{X_cX_s}(\tau) = 0 \tag{16c}$$
$$R_{X_sX_c}(\tau) = 0 \tag{16d}$$
$$R_{XX}(\tau) = 2J_0(w_d\tau) \tag{16e}$$
$$R_{|X|^2|X|^2}(\tau) = 4 + 4J_0^2(w_d\tau) + \frac{4 + 2J_0(2w_d\tau)}{M} = 4 + 4J_0^2(w_d\tau), \quad \text{if } M \to \infty. \tag{16f}$$

Proof: See the appendix ∎

It should be emphasized here that the autocorrelation and cross-correlation functions given by (16a)–(16e) do not depend on the number of sinusoids M, and they match the desired second-order statistics exactly, irrespective of the value of M. This highlights the advantages of the new simulation model over all other existing simulation models. Furthermore, the autocorrelation function of the squared envelope, which involves fourth-order statistics, asymptotically approaches the desired autocorrelation $R_{|g|^2|g|^2}(\tau)$ as the number of sinusoids M approaches infinity, while good approximation has been observed when M is as small as eight. These analytical statistics are confirmed by numerical results in the next section. It is interesting to point out that the autocorrelation of squared fading envelope is very useful for estimating mobile speed which assists handoffs in hierarchical cellular systems [27], power control, etc.

We now present the PDFs of the envelope $|X|$ and phase $\Theta_X(t) = \arctan[X_c(t), X_s(t)]$.

Theorem 2: When M approaches infinity, the envelope $|X|$ is Rayleigh distributed and the phase $\Theta_X(t)$ is uniformly distributed over $[-\pi, \pi)$, and their PDFs are given by

$$f_{|X|}(x) = x \cdot \exp\left(-\frac{x^2}{2}\right), \qquad x \geq 0 \tag{18a}$$
$$f_{\Theta_X}(\theta_X) = \frac{1}{2\pi}, \qquad \theta_X \in [-\pi, \pi). \tag{18b}$$

Proof: Since all the individual sinusoids in the sums of $X_c(t)$ and $X_s(t)$ are statistically independent and identically distributed, according to the central limit theorem [30], when the number of sinusoids M approaches infinity, $X_c(t)$ and $X_s(t)$ become Gaussian random processes. Moreover, since $R_{X_cX_s}(\tau) = 0$ and $R_{X_sX_c}(\tau) = 0$, $X_c(t)$ and $X_s(t)$ are independent. Therefore, the envelope $|X(t)| = \sqrt{X_c^2(t) + X_s^2(t)}$ is Rayleigh distributed, and the phase $\Theta_X(t)$ is uniformly distributed over $[-\pi, \pi)$ [30]. Based on $R_{XX}(\tau = 0) = 2$, one can obtain (18). ∎

Two other important statistical properties associated with fading envelope are the level crossing rate (LCR) and the average fade duration (AFD). The LCR is defined as the rate at which the envelope crosses a specified level in the positive slope, and the AFD is the average time duration that the fading envelope remains below a specified level. Both the LCR and AFD provide important information about the statistics of burst errors [28], [29], which facilitates the design and selection of error-correction technique. It is shown in the following theorem that the LCR and AFD of the new simulator asymptotically match those of Clarke's mathematical reference model [25].

Theorem 3: When M approaches infinity, the LCR $L_{|X|}$ and the AFD $T_{|X|}$ of the new simulator output are given by

$$L_{|X|} = \sqrt{2\pi}\rho f_d e^{-\rho^2} \tag{19a}$$
$$T_{|X|} = \frac{e^{\rho^2} - 1}{\rho f_d \sqrt{2\pi}} \tag{19b}$$

where ρ is the normalized fading envelope level given by $|X|/|X|_{\text{rms}}$, with $|X|_{\text{rms}}$ being the root mean square envelope level.

Proof: When M approaches infinity, the fading envelope is Rayleigh distributed, as shown in *Theorem 2*. Using the same procedure provided in [25], one can prove (19). Details are omitted here for brevity. ∎

Before concluding this section, we have three remarks on the new simulation model.

Remark 1: The initial phase ϕ in the proposed model (14) is to ensure that the model is stationary in the wide sense. The random variable θ (so as α_n) in (15) is to randomize the radian Doppler frequencies $w_d \cos\alpha_n$. This makes the new model different from all the existing Jakes family simulators, such as [10], [16], [18], [19], [21], [22], and [31]. The random variables ψ_n in (14) are intended to ensure that the quadrature components of the fading $X(t)$ are statistically uncorrelated and have equal power. In total, the proposed model needs $M + 2$ random variables, only two more random variables than that of the WSS Jakes' simulator in [22], but it gained significant advantages in the statistical properties.

Remark 2: The proposed simulation model is not unique, there are many other different models with identical or similar statistical properties. These models have different combinations of cosine and sine functions for the quadrature components. Here we list one of them as an example

$$\tilde{X}(t) = \tilde{X}_c(t) + j\tilde{X}_s(t) \tag{20a}$$
$$\tilde{X}_c(t) = \sqrt{\frac{2}{M}} \sum_{n=1}^{M} \sin(\psi_n)\sin(w_d t \sin\alpha_n + \phi) \tag{20b}$$
$$\tilde{X}_s(t) = \sqrt{\frac{2}{M}} \sum_{n=1}^{M} \cos(\psi_n)\sin(w_d t \sin\alpha_n + \phi) \tag{20c}$$

where α_n is defined by (15), and ψ_n, ϕ, and θ are independent and uniformly distributed on $[-\pi, \pi)$ for all n. It can be proved that $\tilde{X}(t)$ has identical statistics to that of $X(t)$, defined by (14).

Remark 3: The new simulation model can be directly used to generate uncorrelated fading waveforms for frequency-selective Rayleigh channels, MIMO channels, and diversity-combing scenarios. Let $X_k(t)$ be the kth Rayleigh fader given by

$$X_k(t) = \sqrt{\frac{2}{M}}\left\{\sum_{n=1}^{M}\cos(\psi_{n,k})\cos\left[w_d t\cos\left(\frac{2\pi n - \pi + \theta_k}{4M}\right) + \phi_k\right] + j\sum_{n=1}^{M}\sin(\psi_{n,k})\cos\left[w_d t\cos\left(\frac{2\pi n - \pi + \theta_k}{4M}\right) + \phi_k\right]\right\} \tag{21}$$

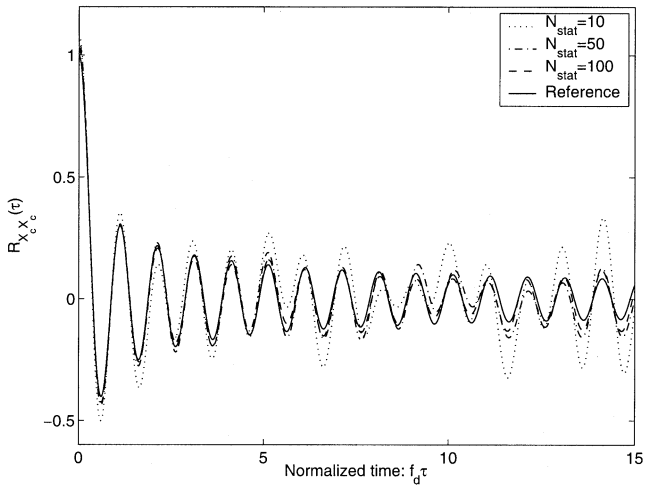

Fig. 1. Autocorrelations of the simulated real-part fading, $X_c(t)$, and reference $g(t)$, where N_{stat} stands for the number of statistical trials.

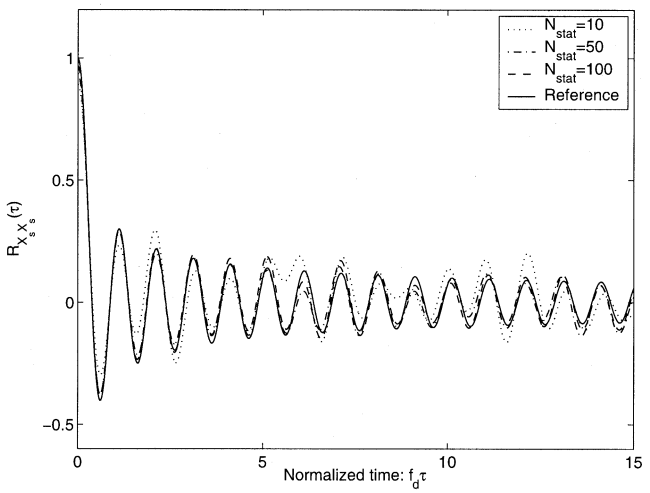

Fig. 2. Autocorrelations of the simulated imaginary-part fading, $X_s(t)$, and reference $g(t)$.

where θ_k, ϕ_k, and $\psi_{n,k}$ are mutually independent and uniformly distributed over $[-\pi, \pi)$ for all n and k. Then, $X_k(t)$ retains all the statistical properties of $X(t)$, which is defined by (14). Furthermore, $X_k(t)$ and $X_l(t)$ are uncorrelated for all $k \neq l$.

IV. Performance Evaluation

The performance evaluation of the proposed fading simulator $X(t)$ defined by (14) is carried out by comparing the corresponding simulation results with those of the mathematical reference model. Throughout the following discussions, the proposed statistical simulator has been implemented by choosing $M = 8$, the normalized sampling period $f_d T_s = 0.025$. The ensemble averages for all the simulation results are based on 10, 50, and 100 random trials which will be indicated in the figures.

A. Evaluation of Correlation Statistics

The simulation results of the autocorrelations of the quadrature components, the cross correlations of the quadrature components, and the autocorrelations of the complex envelope and squared envelope of the simulator output are shown in Figs. 1–6, respectively. The second-order statistics of the mathematical reference model, which are calculated based on (3), are also included in the figures for comparison purposes.

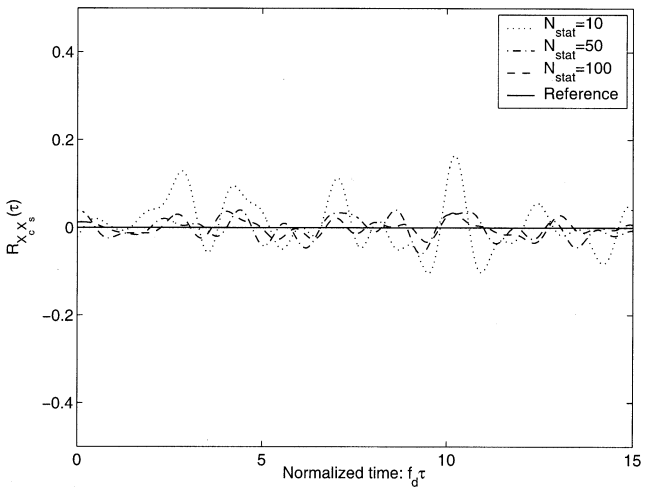

Fig. 3. Cross correlations of the simulated quadrature components of fading $X(t)$ and reference $g(t)$. Note: $R_{X_s X_c}(\tau)$ is almost identical to $R_{X_c X_s}(\tau)$ in our simulations, so we only show one set of the results for brevity.

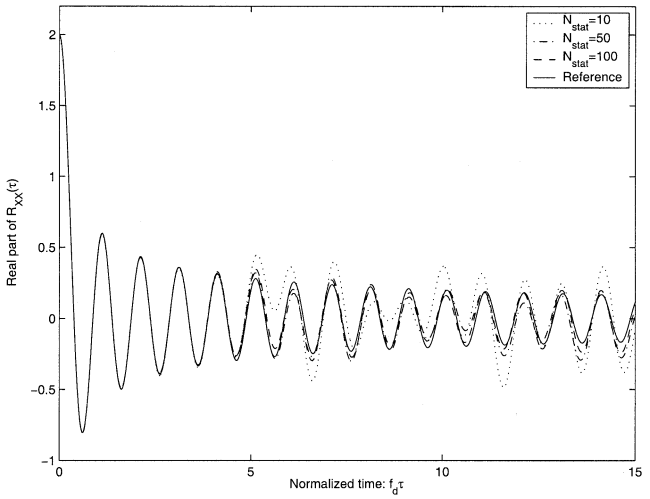

Fig. 4. Real part of the autocorrelations of the simulated complex fading $X(t)$ and reference $g(t)$.

As can be seen from Figs. 1–5, the simulation results show that the autocorrelations of the quadrature components and the complex envelope and the cross correlations of the quadrature components match the desired ones very well, even though M is as small as 8, and the number of statistical trials is as low as 50. If we use more random trials for the ensemble average in the simulations, then the difference between the simulated curves and the desired reference curves will be smaller, until eventually unnoticeable. It is also shown in Fig. 6 that the autocorrelation of the squared envelope of the simulator is very close to the desired one when $M = 8$. If we increase the value of M, then it will be even closer.

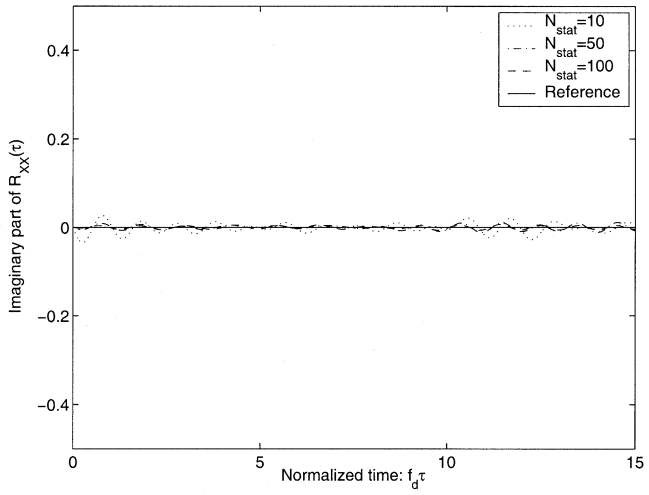

Fig. 5. Imaginary part of the autocorrelations of the simulated complex fading $X(t)$ and reference $g(t)$.

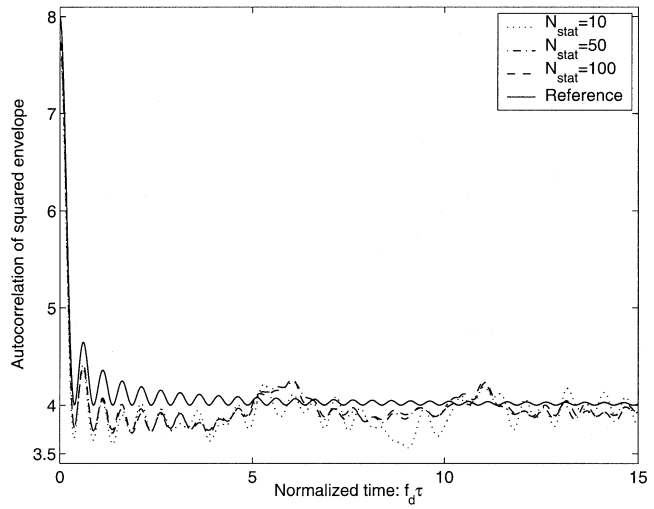

Fig. 6. Autocorrelations of the simulated squared envelope $|X(t)|^2$ and reference $|g(t)|^2$.

B. Evaluation of PDFs of the Envelope and Phase

Figs. 7 and 8 show the PDFs of the fading envelope and the phase of the simulator. It can be seen that the envelope's PDF is in excellent agreement with that of the reference model, even if the number of random trials is small as 10, however, the phase's PDF is a little bit sensitive to the number of random trials, and the more trials, the better, approaching that of the reference model. It is also noted that when $M > 8$, these PDFs will have even better agreement with the desired ones.

C. Evaluation of the LCR and the AFD

The simulation results of the normalized LCR, $L_{|X|}/f_d$, and the normalized AFD, $f_d T_{|X|}$, of the new simulator are shown in Figs. 9 and 10, respectively, where the theoretically calculated LCR and AFD of the reference model are also included in the figures for convenient comparison, indicating good agreement in both cases, even if the number of trials is only 10.

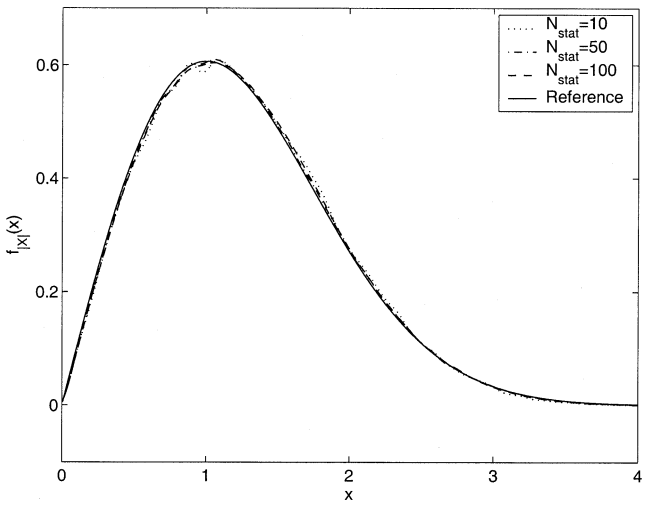

Fig. 7. PDFs of the simulated fading envelope $|X(t)|$ and reference $|g(t)|$.

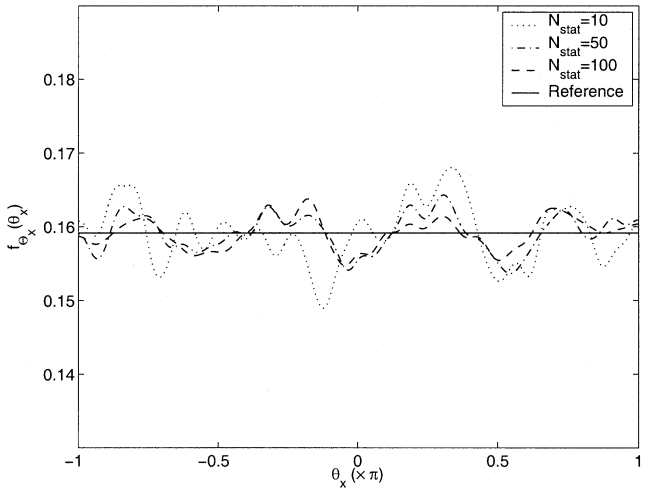

Fig. 8. PDFs of the simulated fading phase $\Theta_X(t)$ and reference $\Theta_g(t)$.

The evaluations of other models mentioned by *Remark 2* have also been conducted by simulations. We found the same level of agreement between simulation results and reference values as those of the simulator $X(t)$ for all the cases. Details are omitted here.

V. Conclusion

In this paper, a new sum-of-sinusoids statistical simulation model was proposed for Rayleigh fading channels. Comparing with Jakes' sum-of-sinusoids deterministic model and its modifications, the new model reintroduces the randomness to the path gain, the Doppler frequency, and the initial phase of the sinusoids to have a nondeterministic simulator with good statistical properties. It has been proven that the autocorrelations of the quadrature components, the cross correlations of the quadrature components, and the autocorrelation of the complex envelope of the new simulator match the desired ones exactly, even if the number of sinusoids used to generate the channel fading is as small as a single-digit integer. It

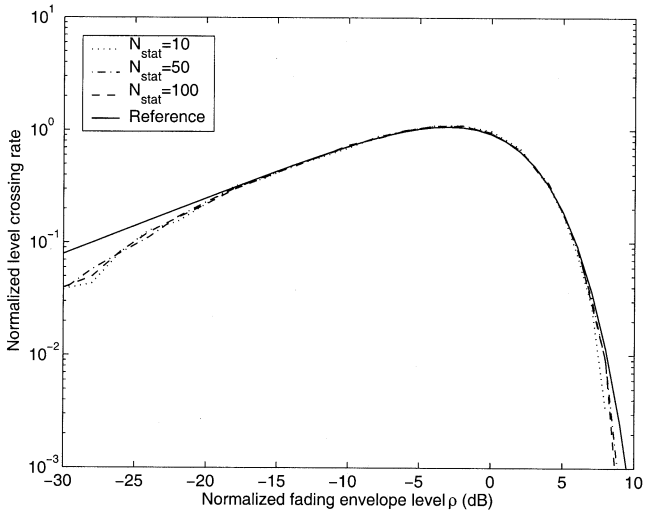

Fig. 9. LCRs of the simulated fading envelope $|X(t)|$ and reference $|g(t)|$.

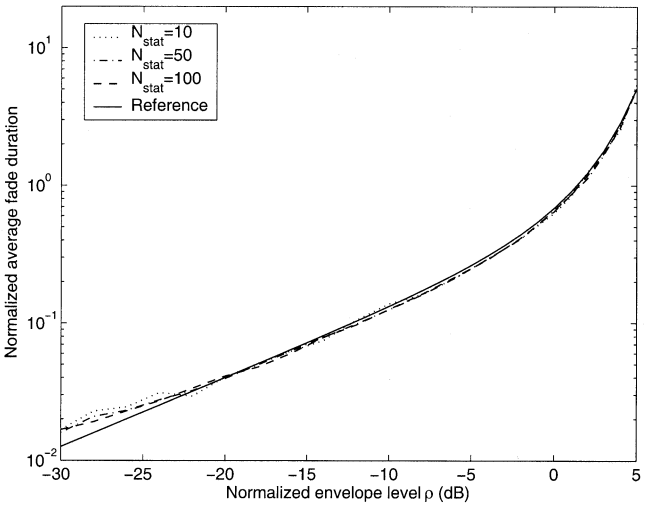

Fig. 10. AFDs of the simulated fading envelope $|X(t)|$ and reference $|g(t)|$.

has also been shown that the autocorrelation of the squared envelope, which contains fourth-order statistics; the PDFs of the fading envelope and phase, the LCR, and the AFD of the new simulator approach those of the mathematical reference model as the number of sinusoids approaches infinity, while good convergence can be reached even when the number of sinusoids and the number of random trials are small. All these statistical properties of the new simulator have been evaluated by extensive simulation results with excellent agreement in all cases except for the fading phase's PDF, which has slower convergence to the desired one. It has been noted that the proposed simulation model can be modified in different ways to have alternative models which have statistical properties unchanged. It has also been pointed out that the new simulation model can be directly used to generate multiple uncorrelated fading waveforms, which are needed to simulate some realistic frequency-selective fading channels, MIMO channels, and diversity-combining scenarios.

APPENDIX

VI. PROOF OF *THEOREM 1*

Proof: Equation (16a) is proved first. The autocorrelation function of the real part of the fading is given to be

$$\begin{aligned}
R_{X_cX_c}(\tau) &= E\left[X_c(t)X_c(t+\tau)\right] \\
&= \frac{4}{M}\sum_{n=1}^{M}\sum_{i=1}^{M} E\left\{\cos(\psi_n)\cos(w_d t\cos\alpha_n+\phi)\right. \\
&\quad \left.\cdot\cos(\psi_i)\cos\left[w_d(t+\tau)\cos\alpha_i+\phi\right]\right\} \\
&= \frac{4}{M}\sum_{n=1}^{M}\sum_{i=1}^{M} E\left\{\cos(\psi_n)\cos(\psi_i)\right\} \\
&\quad \cdot E\{\cos(w_d t\cos\alpha_n+\phi)\cdot\cos[w_d(t+\tau)\cos\alpha_i+\phi]\} \\
&= \frac{1}{M}\left\{\sum_{n=1}^{M} E\left[\cos(w_d\tau\cos\alpha_n)\right]\right\} \\
&= \frac{1}{M}\left\{\sum_{n=1}^{M}\int_{-\pi}^{\pi}\cos\left[w_d\tau\cos\left(\frac{2\pi n-\pi+\theta}{4M}\right)\right]\frac{d\theta}{2\pi}\right\} \\
&= \frac{1}{M}\left\{\sum_{n=1}^{M}\int_{\frac{2\pi n-2\pi}{4M}}^{\frac{2\pi n}{4M}}\cos\left[w_d\tau\cos(\gamma_n)\right]\frac{4M}{2\pi}d\gamma_n\right\} \\
&= \frac{2}{\pi}\int_{0}^{\frac{\pi}{2}}\cos(w_d\tau\cos\gamma)d\gamma \\
&= J_0(w_d\tau)
\end{aligned}$$

where at the fifth equality of the above equations, the integration variable θ was replaced by $\gamma_n = (2\pi n - \pi + \theta)/(4M)$ and $d\theta = 4Md\gamma_n$. This completes the proof of (16a).

Similarly, we can obtain the autocorrelation of the imaginary part of the fading given below

$$\begin{aligned}
R_{X_sX_s}(\tau) &= E\left[X_s(t)X_s(t+\tau)\right] \\
&= \frac{2}{\pi}\int_{0}^{\frac{\pi}{2}}\cos(w_d\tau\cos\gamma)d\gamma \\
&= J_0(w_d\tau).
\end{aligned}$$

We are now in a position to prove (16c) as follows:

$$\begin{aligned}
R_{X_cX_s}(\tau) &= E\left[X_c(t)X_s(t+\tau)\right] \\
&= \frac{2}{M}\sum_{n=1}^{M}\sum_{i=1}^{M} E\left\{\cos(\psi_n)\sin(\psi_i)\right\} \\
&\quad \cdot E\left\{\cos(w_d t\cos\alpha_n+\phi)\sin[w_d(t+\tau)\cos\alpha_i+\phi]\right\} \\
&= \frac{1}{M}\sum_{n=1}^{M} E\left\{\sin(2\psi_n)\right\} \\
&\quad \cdot E\left\{\cos(w_d t\cos\alpha_n+\phi)\sin[w_d(t+\tau)\cos\alpha_n+\phi]\right\} \\
&= 0.
\end{aligned}$$

Moreover, one can validate (16d) in a similar manner.

For (16e), one has

$$\begin{aligned}R_{XX}(\tau) &= E\left\{[X_c(t)+jX_s(t)]\,[X_c(t+\tau)-jX_s(t+\tau)]\right\}\\ &= E\left[X_c(t)X_c(t+\tau)\right]+E\left[X_s(t)X_s(t+\tau)\right]\\ &\quad +jE\left[X_c(t)X_s(t+\tau)\right]-jE\left[X_s(t)X_c(t+\tau)\right]\\ &= 2J_0(w_d\tau).\end{aligned}$$

The proof of (16f) is different and lengthy. A brief outline with some details is given below

$$\begin{aligned}R_{|X|^2|X|^2}(\tau) = E\left[X_c^2(t)X_c^2(t+\tau)\right]+E\left[X_s^2(t)X_s^2(t+\tau)\right]\\ +E\left[X_c^2(t)X_s^2(t+\tau)\right]+E\left[X_s^2(t)X_c^2(t+\tau)\right].\end{aligned}$$

The computation of the first term in the right-hand side of the above equation is shown in detail as follows:

$$\begin{aligned}&E\left[X_c^2(t)X_c^2(t+\tau)\right]\\ &\quad=\frac{16}{M^2}\cdot E\left\{\sum_{n=1}^{M}\cos(\psi_n)\cos(w_dt\cos\alpha_n+\phi)\right.\\ &\qquad\cdot\sum_{i=1}^{M}\cos(\psi_i)\cos(w_dt\cos\alpha_i+\phi)\\ &\qquad\times\sum_{p=1}^{M}\cos(\psi_p)\cos\left[w_d(t+\tau)\cos\alpha_p+\phi\right]\\ &\qquad\left.\cdot\sum_{q=1}^{M}\cos(\psi_q)\cos\left[w_d(t+\tau)\cos\alpha_q+\phi\right]\right\}.\end{aligned}$$

Since the random phases ψ_k and ψ_l are statistically independent for all $k\neq l$, the right-hand side of the above equation is zero except for four different cases: 1) $n=i=p=q$; 2) $n=i$, $p=q$, but $i\neq p$; 3) $n=p$, $i=q$, but $n\neq i$; and 4) $n=q$, $i=p$, but $n\neq i$. So that, $E[X_c^2(t)X_c^2(t+\tau)]$ can be calculated by separating these four different cases.

For the first case, $n=i=p=q$, we have

$$\begin{aligned}&E\left[X_c^2(t)X_c^2(t+\tau)\right]_{1\text{st}}\\ &\quad=\frac{16}{M^2}\sum_{n=1}^{M}E\left[\cos^4(\psi_n)\right]\\ &\qquad\times E\left\{\cos^2(w_dt\cos\alpha_n+\phi)\cdot\cos^2\left[w_d(t+\tau)\cos\alpha_n+\phi\right]\right\}\\ &\quad=\frac{16}{M^2}\left\{\sum_{n=1}^{M}\frac{3}{8}\cdot E\left[\frac{1+\cos(2w_dt\cos\alpha_n+2\phi)}{2}\right.\right.\\ &\qquad\left.\left.\cdot\frac{1+\cos\left[2w_d(t+\tau)\cos\alpha_n+2\phi\right]}{2}\right]\right\}\\ &\quad=\frac{16}{M^2}\left\{\sum_{n=1}^{M}\left[\frac{3}{32}+\frac{3}{64}\cdot E\left[\cos(2w_d\tau\cos\alpha_n)\right]\right]\right\}\\ &\quad=\frac{1}{M^2}\left\{\frac{3M}{2}+\frac{3M}{4}J_0(2w_d\tau)\right\}\\ &\quad=\frac{3}{2M}+\frac{3}{4M}J_0(2w_d\tau)\end{aligned}$$

where the last step of the above equation used the following result:

$$\sum_{n=1}^{M}E\left[\cos(2w_n\tau)\right]=MJ_0(2w_d\tau).$$

For the second case, $n=i$, $p=q$, but $i\neq p$, then

$$\begin{aligned}&E\left[X_c^2(t)X_c^2(t+\tau)\right]_{2\text{nd}}\\ &\quad=\frac{16}{M^2}\left\{\sum_{n=1}^{M}E\left[\cos^2(\psi_n)\cos^2(w_dt\cos\alpha_n+\phi)\right]\right.\\ &\qquad\left.\cdot\sum_{p=1}^{M}E\left(\cos^2(\psi_p)\cos^2\left[w_d(t+\tau)\cos\alpha_p+\phi\right]\right)\right\}\\ &\quad=\frac{16}{M^2}\left[\sum_{n=1}^{M}\frac{1}{2}\cdot\frac{1}{2}\right]\left[\sum_{p=1}^{M}\frac{1}{2}\cdot\frac{1}{2}\right]\\ &\quad=1.\end{aligned}$$

For the third case, $n=p$, $i=q$, but $n\neq i$, then

$$\begin{aligned}&E\left[X_c^2(t)X_c^2(t+\tau)\right]_{3\text{rd}}\\ &\quad=\frac{16}{M^2}\left\{\sum_{n=1}^{M}E\left[\cos^2(\psi_n)\cos(w_dt\cos\alpha_n+\phi)\right.\right.\\ &\qquad\left.\times\cos\left[w_d(t+\tau)\cos\alpha_n+\phi\right]\right]\\ &\qquad\times\sum_{i=1}^{M}E\left[\cos^2(\psi_i)\cos(w_dt\cos\alpha_i+\phi)\right.\\ &\qquad\left.\left.\times\cos\left[w_d(t+\tau)\cos\alpha_i+\phi\right]\right]\right\}\\ &\quad=\frac{16}{M^2}\left\{\sum_{n=1}^{M}\frac{1}{4}\cdot E\left[\cos(w_d\tau\cos\alpha_n)\right]\right\}^2\\ &\quad=\frac{16}{M^2}\left[\frac{MJ_0(w_d\tau)}{4}\right]^2\\ &\quad=J_0^2(w_d\tau).\end{aligned}$$

For the fourth case, $n=q$, $i=p$, but $n\neq i$, similarly to the third case, one can prove

$$E\left[X_c^2(t)X_c^2(t+\tau)\right]_{4\text{th}}=J_0^2(w_d\tau).$$

Since these four cases are exclusive and exhaustive for $E[X_c^2(t)X_c^2(t+\tau)]$ being nonzero, overall we have

$$\begin{aligned}E\left[X_c^2(t)X_c^2(t+\tau)\right] &= E\left[X_c^2(t)X_c^2(t+\tau)\right]_{1\text{st}}\\ &\quad+E\left[X_c^2(t)X_c^2(t+\tau)\right]_{2\text{nd}}\\ &\quad+E\left[X_c^2(t)X_c^2(t+\tau)\right]_{3\text{rd}}\\ &\quad+E\left[X_c^2(t)X_c^2(t+\tau)\right]_{4\text{th}}\\ &= 1+2J_0^2(w_d\tau)+\frac{3}{2M}+\frac{3}{4M}J_0(2w_d\tau).\end{aligned}$$

This completes the computation of $E[X_c^2(t)X_c^2(t+\tau)]$.

Using the same procedure shown above, after some statistical and algebraic manipulations, one can obtain the following results:

$$\begin{aligned}E\left[X_s^2(t)X_s^2(t+\tau)\right] &= 1+2J_0^2(w_d\tau)+\frac{3}{2M}+\frac{3}{4M}J_0(2w_d\tau)\\ E\left[X_c^2(t)X_s^2(t+\tau)\right] &= 1+\frac{1}{2M}+\frac{1}{4M}J_0(2w_d\tau)\\ E\left[X_s^2(t)X_c^2(t+\tau)\right] &= 1+\frac{1}{2M}+\frac{1}{4M}J_0(2w_d\tau).\end{aligned}$$

Therefore

$$\begin{aligned}R_{|X|^2|X|^2}(\tau) &= 4+4J_0^2(w_d\tau)+\frac{4+2J_0(2w_d\tau)}{M}\\ &= 4+4J_0^2(w_d\tau),\quad\text{when } M\to\infty.\end{aligned}$$

This completes the proof of *Theorem 1*. ■

ACKNOWLEDGMENT

The authors wish to thank Professor N. C. Beaulieu for suggesting changes to the original manuscript that improved it immensely. The authors are also grateful to the anonymous reviewers for their helpful comments.

REFERENCES

[1] R. H. Clarke, "A statistical theory of mobile-radio reception," *Bell Syst. Tech. J.*, pp. 957–1000, Jul.–Aug. 1968.
[2] M. J. Gans, "A power-spectral theory of propagation in the mobile-radio environment," *IEEE Trans. Veh. Technol.*, vol. VT-21, pp. 27–38, Feb. 1972.
[3] T. Aulin, "A modified model for the fading signal at a mobile radio channel," *IEEE Trans. Veh. Technol.*, vol. VT-28, pp. 182–203, Aug. 1979.
[4] H. Hashemi, "Simulation of the urban radio propagation channel," *IEEE Trans. Veh. Technol.*, vol. VT-28, pp. 213–225, Aug. 1979.
[5] A. A. M. Saleh and R. A. Valenzuela, "A statistical model for indoor multipath propagation," *IEEE J. Select. Areas Commun.*, vol. SAC-5, pp. 128–137, Feb. 1987.
[6] W. C. Jakes, *Microwave Mobile Communications*. Piscataway, NJ: IEEE Press, 1994.
[7] W. R. Braun and U. Dersch, "A physical mobile radio channel model," *IEEE Trans. Veh. Technol.*, vol. 40, pp. 472–482, May 1991.
[8] P. Hoeher, "A statistical discrete-time model for the WSSUS multipath channel," *IEEE Trans. Veh. Technol.*, vol. 41, pp. 461–468, Nov. 1992.
[9] S. A. Fechtel, "A novel approach to modeling and efficient simulation of frequency-selective fading radio channels," *IEEE J. Select. Areas Commun.*, vol. 11, pp. 422–431, Apr. 1993.
[10] P. Dent, G. E. Bottomley, and T. Croft, "Jakes fading model revisited," *Electron. Lett.*, vol. 29, no. 13, pp. 1162–1163, June 1993.
[11] U. Dersch and R. J. Ruegg, "Simulations of the time and frequency selective outdoor mobile radio channel," *IEEE Trans. Veh. Technol.*, vol. 42, pp. 338–344, Aug. 1993.
[12] D. Verdin and T. C. Tozer, "Generating a fading process for the simulation of land-mobile radio communications," *Electron. Lett.*, vol. 29, pp. 2011–2012, Nov. 1993.
[13] P. M. Crespo and J. Jimenez, "Computer simulation of radio channels using a harmonic decomposition technique," *IEEE Trans. Veh. Technol.*, vol. 44, pp. 414–419, Aug. 1995.
[14] K.-W. Yip and T.-S. Ng, "Discrete-time model for digital communications over a frequency-selective Rician fading WSSUS channel," *Inst. Elect. Eng. Proc. Commun.*, vol. 143, pp. 37–42, Feb. 1996.
[15] ——, "Karhunen-Loeve expansion of the WSSUS channel output and its application to efficient simulation," *IEEE J. Select. Areas Commun.*, vol. 15, pp. 640–646, May 1997.
[16] M. Patzold, U. Killat, F. Laue, and Y. Li, "On the statistical properties of deterministic simulation models for mobile fading channels," *IEEE Trans. Veh. Technol.*, vol. 47, pp. 254–269, Feb. 1998.
[17] M. Patzold and F. Laue, "Statistical properties of Jakes' fading channel simulator," in *Proc. IEEE VTC'98*, 1998, pp. 712–718.
[18] Y. X. Li and X. Huang, "The generation of independent Rayleigh faders," in *Proc. IEEE ICC'00*, 2000, pp. 41–45.
[19] Y. B. Li and Y. L. Guan, "Modified Jakes model for simulating multiple uncorrelated fading waveforms," in *Proc. IEEE ICC'00*, 2000, pp. 46–49.
[20] K.-W. Yip and T.-S. Ng, "A simulation model for Nakagami-m fading channels, $m < 1$," *IEEE Trans. Commun.*, vol. 48, pp. 214–221, Feb. 2000.
[21] M. Patzold, R. Garcia, and F. Laue, "Design of high-speed simulation models for mobile fading channels by using table look-up techniques," *IEEE Trans. Veh. Technol.*, vol. 49, pp. 1178–1190, July 2000.
[22] M. F. Pop and N. C. Beaulieu, "Limitations of sum-of-sinusoids fading channel simulators," *IEEE Trans. Commun.*, vol. 49, pp. 699–708, Apr. 2001.
[23] E. Chiavaccini and G. M. Vitetta, "GQR models for multipath Rayleigh fading channels," *IEEE J. Select. Areas Commun.*, vol. 19, pp. 1009–1018, June 2001.
[24] C. Xiao, Y. R. Zheng, and N. C. Beaulieu, "Second-order statistical properties of the WSS Jakes' fading channel simulator," *IEEE Trans. Commun.*, vol. 50, pp. 888–891, June 2002.
[25] G. L. Stuber, *Principles of Mobile Communication*, 2nd ed. Norwell, MA: Kluwer, 2001.
[26] I. S. Gradshteyn and I. M. Ryzhik, *Table of Integrals, Series, and Products*, 6th ed, A. Jeffrey, Ed. New York: Academic, 2000.
[27] C. Xiao, K. D. Mann, and J. C. Olivier, "Mobile speed estimation for TDMA-based hierarchical cellular systems," *IEEE Trans. Veh. Technol.*, pp. 981–991, July 2001.
[28] K. Ohtani, K. Daikoku, and H. Omori, "Burst error performance encountered in digital land mobile radio channel," *IEEE Trans. Veh. Technol.*, vol. VT-23, pp. 156–160, Jan. 1981.
[29] J. M. Morris, "Burst error statistics of simulated Viterbi decoded BPSK on fading and scintillating channels," *IEEE Trans. Commun.*, vol. 40, pp. 34–41, 1992.
[30] J. G. Proakis, *Digital Communications*, 4th ed. New York: McGraw-Hill, 2001.
[31] Y. X. Li and X. Huang, "The simulation of independent Rayleigh faders," *IEEE Trans. Commun.*, vol. 50, pp. 1503–1514, Sept. 2002.
[32] Y. R. Zheng and C. Xiao, "Improved models for the generation of multiple uncorrelated Rayleigh fading waveforms," *IEEE Commun. Lett.*, vol. 6, pp. 256–258, June 2002.

Yahong Rosa Zheng received the B.S. degree from the University of Electronic Science and Technology of China, Chengdu, China, in 1987, the M.S. degree from Tsinghua University, Beijing, China, in 1989, and the Ph.D. degree from Carleton University, Ottawa, ON, Canada, in 2002, all in electrical engineering.

From 1989 to 1994, she was a Senior Member of Scientific Staff with the Peony Electronic Group, Beijing, China. From 1994 to 1997, she held positions with GPS Solutions at Sagem Australasia Pty. Ltd., Sydney, Australia, and Polytronics Pty. Ltd., Toronto, ON, Canada. Currently, she is an NSERC Postdoctoral Fellow with the Department of Electrical Engineering, University of Missouri, Columbia. Her research interests include digital signal processing algorithms, array signal processing, channel estimation, and modeling for wireless communications. She has published a number of papers in international journals and conferences, and received two patents in China.

Chengshan Xiao (M'99–SM'02) received the B.S. degree from the University of Electronic Science and Technology of China, Chengdu, China, in 1987, the M.S. degree from Tsinghua University, Beijing, China, in 1989, and the Ph.D. degree from the University of Sydney, Sydney, Australia, in 1997, all in electrical engineering.

From 1989 to 1993, he was on the Research Staff and then became a Lecturer with the Department of Electronic Engineering, Tsinghua University, Beijing, China. From 1997 to 1999, he was a Senior Member of Scientific Staff at Nortel Networks, Ottawa, ON, Canada. From 1999 to 2000, he was an Assistant Professor with the Department of Electrical and Computer Engineering, University of Alberta, Edmonton, AB, Canada. Currently, he is an Assistant Professor with the Department of Electrical and Computer Engineering, University of Missouri, Columbia. His research interests include wireless communications, signal processing, and multidimensional and multirate systems. He has published extensively in these areas. Some of his algorithms have been implemented into Nortel's base station radios with successful technical field trials and network integration.

Dr. Xiao is an Associate Editor for the IEEE TRANSACTIONS ON WIRELESS COMMUNICATIONS, the IEEE TRANSACTIONS ON VEHICULAR TECHNOLOGY, the IEEE TRANSACTIONS ON CIRCUITS AND SYSTEMS—I, and the international journal of *Multidimensional Systems and Signal Processing*.